SIMULATION OF THE DC CONDUCTANCE OF BALLISTIC QUANTUM DEVICES

Edval J. P. Santos

Laboratory for Devices and Nanostructures - Departamento de Eletrônica e Sistemas,
Universidade Federal de Pernambuco, Caixa Postal 7800, 50711-970 Recife-PE, Brazil

ABSTRACT

Simulation programs for electron transport makes possible to evaluate the performance of advanced electron devices structures before they are fabricated. For devices in the nanometer-range scale, quantum physics cannot be ignored. New device behavior is observed as the confinement of charge carriers makes the dual nature of the carriers even more explicit. As we move towards smaller and smaller devices, we get to a development crossroad. In one side, there is the development of novel architectures to use the hundreds of million transistors that can be integrated, on the other side one can try to find new devices which can exploit the quantum nature of the charge carriers confined in wires a few atoms wide. In this paper, we present the computer program we developed, to simulate the DC conductance of quantum devices.

INTRODUCTION

The continued development of microelectronics technology is bringing us closer to the atomic level. As we move towards smaller and smaller devices, we get to a development crossroad. In one side, there is the development of novel architectures to use the hundreds of million transistors that can be integrated; on the other side one can try to find new devices which can exploit the quantum nature of the charge carriers confined in wires a few atoms wide. Simulation programs for electron transport makes possible to evaluate the performance of electron devices before they are manufactured. For devices in the nanometer-range scale, quantum physics cannot be ignored. New device behaviors are observed as the confinement of charge carriers make the dual nature of the carriers even more explicit. Over the years many different effects have been discovered, such as: quantized hall effects, resonant tunneling, quantized conductance, quantum interference, localization, excess noise. The electrons participating on the current flow have energy near the Fermi energy. Therefore, the Fermi energy is a unit of energy at this scale, and the Fermi wavelength is the characteristic dimension used to classify the quantum device as 2-, 1-, 0-D, depending whether the system has one, two or three dimensions of the order of this characteristic length. Quantum effects are observed when one of the dimensions of the nanostructure is of the order of the Fermi wavelength. A two-dimensional quantum structure is a interface, confinement effects in such systems were first observed in high quality FETs (GaAs/AlGaAs), and this research led to the discovery of the quantum Hall effect. A one-dimensional nanostructure is a quantum wire, in this system one observes the quantization of the electrical conductance. A zero-dimensional device is a quantum dot, in this system one observes single electron effects, and quantum capacitance effects. Examples of quantum devices are quantum

constrictions, Aharonov-Bohm rings, electronic Mach-Zender interferometers, quantum dots, among others. It may be that none of these devices yield something useful, and one has to be careful not to be tempted by false advertising (1). However, a better understanding of the physics of such devices is important for the evaluation of its possible use. For this reason, a simulation program to study the electrical characteristics of quantum devices is an interesting tool to examine the electrical behavior of different devices before making them in the clean room. In this paper, our simulation program for the DC conductance of quantum devices is presented.

ELECTRON TRANSPORT

The transport properties of traditional devices, e.g. MOSFET, bipolar transistor, are usually calculated within the semi-classical approach, which has been quite successful over the years (2), (3). In this approach, the movement of the electron cloud is described by the Boltzmann equation. The electron is considered like a classical billiard ball, while the scattering event is quantum. It is assumed that the scattering event is localized in space and time, and that its duration is much shorter then the time between two collision events.

In quantum devices, the electron can not be considered like a billiard ball anymore, it is necessary to apply a full quantum description to describe correctly its flow through the device (4). For example, to calculate the current density, one can solve Schrödinger equation to obtain the wavefunctions, which are used in Equation 1 to calculate the requested property.

$$\vec{J} = -i\frac{e\hbar}{2m}[\Psi^*\nabla\Psi - \Psi\nabla\Psi^*] \tag{1}$$

where, $i^2 = -1$, e is the electron charge, m is the electron effective mass.

As the electron flows through the device, it may suffer scattering events. These events are classified as elastic or inelastic. In elastic scattering, the wavefunction preserves its phase coherence. When electron transport is coherent, the quantum device is said to be ballistic (5). Inelastic scattering does not preserve phase coherency, in this case the transport is classified as diffusive.

Electrical engineers are very much interested on the dependence of the current with applied electric potential difference on device terminals, because this relationship will determine the possible application of the device. The slope of the curve on $I \times V$ plots is the conductance. In the quantum regime, Landauer (6) has shown that the conductance is related to the transmission probability, as given by Equation 2.

$$G = g_s G_Q \sum |T(E)| \tag{2}$$

where $G_Q = e^2/h = 3.873 \times 10^{-5} S$ is the conductance quantum, and $g_s = 2$ is the spin degeneracy. $T(E)$ is the quantum transmission probability, $|T(E)| = 1$ for open channels, and $|T(E)| = 0$ for closed channels. As the energy, E, changes, channels will open or close. This step-like behavior of the conductance is observed experimentally.

In a semiconductor, one has to include the valley degeneracy, g_v. This will modify the conductance formula, as indicated in Equation 3. The numerical value of g_v has a dependence on the cross-sectional shape (13).

$$G = g_v g_s G_Q \sum |T(E)| \tag{3}$$

To calculate the Landauer conductance, the quantum transmission probability must be obtained. This is achieved by calculating the electron wavefunctions. The wavefunctions are solutions of the Schrödinger equation ($H\Psi = E\Psi$). It is necessary to have a Hamiltonian, H, describing the quantum device. The tight-binding Hamiltonian is such a model Hamiltonian (7), (8), (9), (10). In this Hamiltonian, a set of wavefunctions, $\{\Psi_l\}$ ($l = l_1 l_2 l_3$), each localized at different site, form an orthonormal basis ($\int \Psi_l^* \Psi_m dr = \delta_{lm}$) for the solutions. The tight-binding Hamiltonian has a simple matrix representation (see Equation 4), hence it is quite suitable for numerical calculations.

$$\underline{H} = \begin{pmatrix} \epsilon_1 & V_{12} & \dots & V_{1,N\times M} \\ V_{21} & \epsilon_2 & \dots & V_{2,N\times M} \\ . & . & . & . \\ . & . & . & . \\ . & . & . & . \\ V_{N\times M,1} & V_{N\times M,2} & \dots & \epsilon_{N\times M} \end{pmatrix} \tag{4}$$

where ϵ_l is the eigenenergy at site l, and V_{lm} is the interaction energy between site l and site m.

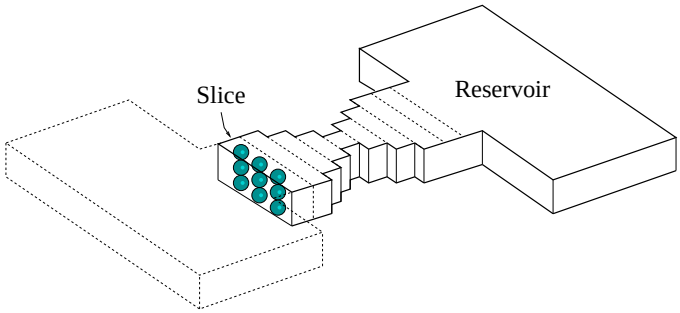

Fig. 1. Quantum device divided in slices for the simulation of quantum transport. The device is connected to two reservoirs.

For the purpose of this calculation, only first-neighbor interaction is considered. This approximation is made among slices, and among sites within a slice. Schrödinger equation is now written as presented in Equation 5.

$$\begin{pmatrix} \underline{H}_{11} & \underline{V}_{12} & 0 & \dots & 0 \\ \underline{V}_{21} & \underline{H}_{22} & \underline{V}_{23} & \dots & 0 \\ 0 & \underline{V}_{32} & \underline{H}_{33} & \dots & 0 \\ . & . & . & & . \\ . & . & . & & . \\ . & . & . & & . \\ 0 & 0 & 0 & \dots & \underline{H}_{NN} \end{pmatrix} \begin{pmatrix} \underline{\Psi}_1 \\ \underline{\Psi}_2 \\ \underline{\Psi}_3 \\ . \\ . \\ . \\ \underline{\Psi}_N \end{pmatrix} = E \begin{pmatrix} \underline{\Psi}_1 \\ \underline{\Psi}_2 \\ \underline{\Psi}_3 \\ . \\ . \\ . \\ \underline{\Psi}_N \end{pmatrix} \tag{5}$$

Each element of the matrix, $\underline{H}_{ij}$, is a matrix itself. Diagonal elements is related to an individual slice, and elements off-diagonal represent the interaction among slices. There are many techniques to calculate the wavefunctions (11). In this paper, we apply the recursive Green-function technique, as indicated in Equation 6.

$$(E\underline{I} - \underline{H})\underline{G} = \underline{I} \tag{6}$$

where $\underline{I}$ is the identity matrix, and $\underline{G}$ is the Green function matrix.

The problem now can be solved using a matrix package like LAPACK or directly in a MATLAB-like program.

The algorithm

To setup the calculation, two extra slices are added, slice 0 and slice $N+1$, they represent the reservoirs (see Figure 2). To calculate the transmission probability, the wavefunction is calculated first at slice 0, by solving the eigenvalue problem using the $2M \times 2M$ system shown in Equation 7. The first line of the matrix is Schrödinger equation, and the second line is the condition $\Psi_i = e^{ika}\Psi_{i-1} = \lambda\Psi_{i-1}$, where a is the lattice parameter.

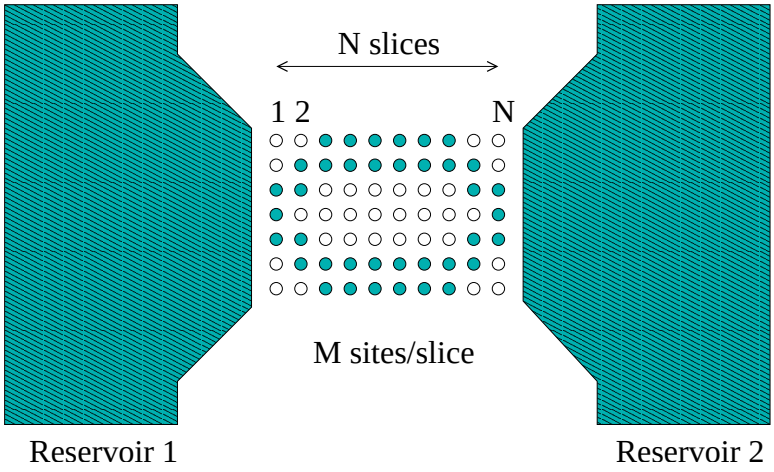

Fig. 2. Quantum device connecting two reservoirs. The device is divided in N slices, with M sites each, for a total of $N \times M$ sites.

$$\begin{pmatrix} \underline{V}_{i,i+1}^{-1}(E - \underline{H}_{i,i}) & -\underline{V}_{i,i+1}^{-1}\underline{V}_{i,i-1} \\ \underline{I} & \underline{0} \end{pmatrix} \begin{pmatrix} \underline{\Psi}_i \\ \underline{\Psi}_{i-1} \end{pmatrix} = \lambda \begin{pmatrix} \underline{\Psi}_i \\ \underline{\Psi}_{i-1} \end{pmatrix} \tag{7}$$

The solution of this eigenvalue problem yields two sets of eigenfunctions and eigenvalues. One set propagates to the left, and the other to the right. The eigenfunction can be combined in a matrix. The left-going waves is represented as $\underline{U}(-)$ and the right-going waves is represented as $\underline{U}(+)$. To decide the direction of propagation, one checks the eigenvalues associated with the eigenfunction. If the eigenvalue is real and less then one, it is a right-going evanescent mode, a real eigenvalue larger then one is a left-going evanescent mode. For complex eigenvalue, one should check the imaginary part. If the imaginary part of the eigenvalue is positive the wavefunction is propagating to the right. A negative imaginary part is a wavefunction propagating to the left (9). Equivalently, one can combine the eigenvalues in a diagonal matrix form, $\underline{\Lambda}(-)$ for the left-going waves and $\underline{\Lambda}(+)$ for the right-going waves. These wavefunctions are used to calculate the initial Green function $\underline{G}_{00}$

$$\underline{G}_{00} = [E\underline{I} - \underline{H}_0 - t(U(-)\Lambda(-)^{-1}U(-)^{-1})]^{-1} \tag{8}$$

Now, the scattering effect is included. At the zeroth slice, the wavefunction has two

components, one incident and the other reflected ($\Psi_0 = \Psi_0^{(+)} + \Psi_0^{(-)}$). At the $N+1$-slice there is only the transmitted component ($\Psi_{N+1} = \Psi_{N+1}^{(+)}$).

$$\begin{pmatrix} \underline{\Psi}_0 \\ \underline{\Psi}_1 \\ . \\ . \\ . \\ \underline{\Psi}_{N+1} \end{pmatrix} = \begin{pmatrix} \underline{G}_{00} & \underline{G}_{01} & \cdots & \underline{G}_{0,N+1} \\ \underline{G}_{10} & \underline{G}_{11} & \cdots & \underline{G}_{0,N} \\ . & . & . & . \\ . & . & . & . \\ . & . & . & . \\ \underline{G}_{N+1,0} & \underline{G}_{N+1,1} & \cdots & \underline{G}_{N+1,N+1} \end{pmatrix} \begin{pmatrix} \underline{V}_0 \\ 0 \\ . \\ . \\ . \\ 0 \end{pmatrix} \tag{9}$$

The Green function can be thought as making the connection between the two reservoirs (see Equation 10). Its calculation can be used to get the transmission probability.

$$\underline{\Psi}_{N+1}^{(+)} = \underline{G}_{N+1,0}\underline{V}_0 \tag{10}$$

The Hamiltonian matrix of a slice is constructed with $H_{ii} = V(slice, i) - 4t$, and $H_{i,i+1} = H_{i+1,i} = -t$, where t is the coupling strength between sites (8). The Hamiltonian matrix, $\underline{H}$, is $M \times M$.

$$\underline{H}_i = \begin{pmatrix} V_1 - 4t & -t & 0 & \cdots & 0 \\ -t & V_2 - 4t & -t & \cdots & 0 \\ 0 & -t & V_3 - 4t & \cdots & 0 \\ . & . & . & & . \\ . & . & . & & . \\ . & . & . & & . \\ 0 & 0 & 0 & \cdots & V_M - 4t \end{pmatrix} \tag{11}$$

where V_i in the diagonal is the local potential energy profile at a given slice.

The calculation starts with $\underline{G}_{00}$ and the device is constructed recursively (10) slice by slice, using Equations 12, until the $N+1$ slice is reached. As the slices are added, the new value of the Green function is calculated as follows:

$$\begin{aligned} \underline{G}_{i+1,i+1} &= [E\underline{I} - \underline{H}_i - t^2\underline{G}_{i,i}]^{-1} \\ \underline{G}_{i+1,0} &= -t\underline{G}_{i+1,i+1}\underline{G}_{i,0} \end{aligned} \tag{12}$$

Finally, at the second reservoir

$$\begin{aligned} \underline{G}_{N+1,N+1} &= [E\underline{I} - \underline{H}_N - t\underline{U}(+)\underline{\Lambda}(+)\underline{U}^{-1}(+) - t^2\underline{G}_{N,N}]^{-1} \\ \underline{G}_{N+1,0} &= -t\underline{G}_{N+1,N+1}\underline{G}_{N,0} \end{aligned} \tag{13}$$

The transmission probability is related to the Green function.

$$T(E)_{ij} = -t[\underline{U}^{-1}(+)\underline{G}(E)_{N+1,0}(\Lambda(-) - \Lambda(+))\underline{U}(+)]_{ij} \tag{14}$$

where, the channel velocity are assumed the same for all channels.

Finally, the Landauer formula is used to calculate the DC conductance. The simulation program has the following steps:

1. Setup the geometry;

2. Initialize the simulation parameters;
3. Calculate the Green function matrix:
 (a) **while** E > Emin
 (b) slice = 1;
 (c) CalcG0;
 (d) slice = 2;
 (e) **while** slice < N
 (f) CalcGplus1;
 (g) slice = slice + 1;
 (h) **end**
 (i) slice = N;
 (j) GNplus1;
 (k) Condut;
 (l) E = E - Estep;
 (m) **end**
4. Plot results.

We have sucessfully implemented this algorithm in C using CLAPACK, and with MATLAB.

RESULTS

The nanostructure to be simulated is stored in matrix format, where each column represents a layer. The lattice parameter is about $0.25nm$. Typical nanometer scale device is under $100nm$ in at least one dimension ($M < 400$). The length of the nanostructure is somewhere between $10nm$ and $1000nm$ ($N = 40 - 4000$).

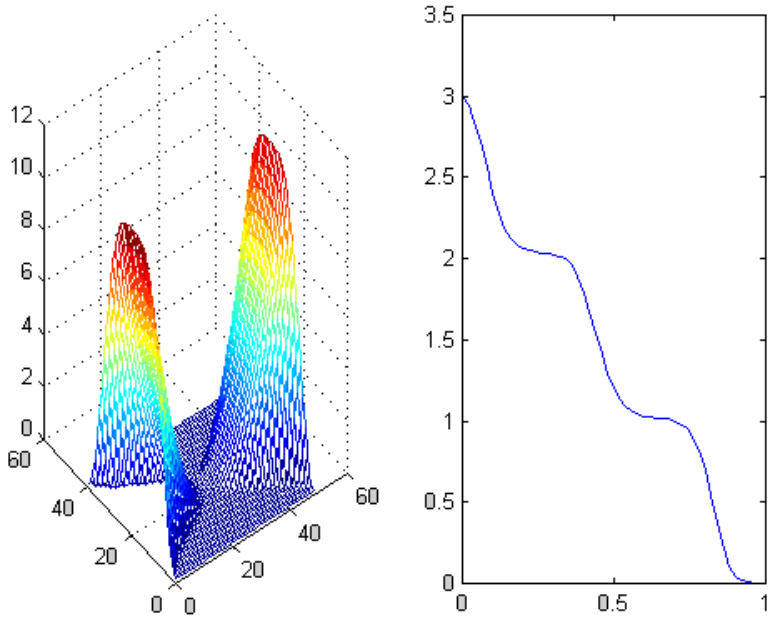

Fig. 3. Simulation of a quantum constriction as it closes the conduction channels. This can be thought as a gate-all-around quantum device, where the gate voltage is used to open or close the channels. The plots is generated with MATLAB.

The program is used to calculate the conductance through a quantum constriction

$10nm$ wide. A voltage applied around the constriction is used to close the conductance channels. The result of the simulation is the same with both programs (C and MATLAB). It is shown in the plots of Figure 3, the shape of the potential surface on the left, and the resulting dependence of the conductance with the voltage on the right. As the barrier rises, the constriction closes and the conductance decreases in a step-like behavior, as expected. For the simulated device, $N = 40$, $M = 48$, and $t = 1.62$.

The simulation is carried out with a Pentium $133MHz$ microcomputer with 32Mb RAM. Such ballistic quantum devices can be manufactured using metal layers (12) or with SOI technology (13),(14),(15), (16), (17) among others.

CONCLUSIONS

This work has presented the numerical program we have written for the simulation of the DC conductance of ballistic quantum devices. The program is based on the recursive Green function technique to connect the device terminals and calculate the quantum transmission probability. To test the program a quantum wire with a constriction or a quantum point contact is simulated. The simulated conductance yields the step-like behavior observed in real world nanodevices. The advantage of this approach is that it should be possible to simulate different device geometries easily. The slice-by-slice calculation reduces the computer power and memory needs.

ACKNOWLEDGMENTS

The author would like to thank Prof. Jean-Pierre Colinge, who provided the computing facility at Université Catholique at Louvain-La-Neuve in the beginning of this work. The author is also grateful to the *Instituto do Milênio*–CNPq, Brazilian Agency.

REFERENCES

1. Rolf Landauer, *Physica A*, **168**, 75 (1990).
2. David K. Ferry and Robert O. Grondin, *Physics of submicron devices*, Plenum Press, New York (1991)
3. Richard L. Liboff, *Kinetic theory: classical, quantum, and relativistic descriptions*, p. 130, Prentice-Hall Advanced Reference Series, New Jersey (1990).
4. H. Baranger and A. Douglas Stone, *Phys. Rev. B*, **40**, 8169 (1989).
5. A. D. Stone, in *Physics of Nanostructures*, p 65, edited by J. H. Davies and A. R. Long, Proceedings of the 38th Scotish Universities Summer School in Physics, Institute of Physics, Bristol (1992)
6. Rolf Landauer, *IBM J. Res. Develop.*, **1**, 223 (1957); *Phil. Mag.*, **21**, 863 (1970).
7. Felix A. Buot, *Physics Reports*, **234**, 73-174 (1993).
8. T. Ando, *Phys. Rev. B*, **44**, 8017-8027 (1991).
9. K. Nikolić and A. MacKinnon, *Phys. Rev. B*, **50**, 11008-11017 (1994).
10. A. MacKinnon, *Z. Phys. B*, **59**, 385 (1985).
11. D. K. Ferry and C. Jacoboni, editors, "Quantum transport in semiconductors", Plenum Press, New York (1992).
12. G. M. Mikhailov, L. I. Aparshina, A. V. Chernykh, S. V. Dubonos, Yu I. Koval, and I. V. Malikov, *Nanotechnology*, **9**, 1-5 (1998).
13. Y. Nakajima, Y. Takahashi, S. Horiguchi, K. Iwadate, H. Namatsu, K. Kurihara, and M. Tabe, *Jpn. J. Appl. Phys.*, **34**, 1309-1314 (1995).
14. X. Baie, J. P. Colinge, *Solid State Electron.*, **42**, 499-504 (1998)
15. X. Baie, J. P. Colinge, V. Bayot, and E. Grivei, *Solid State Electron.*, **39**, 49-51 (1996)
16. X. H. Tang, X. Baie, and J. P. Colinge, *Jpn J. Appl. Phys.*, **37**, 1591-1593 (1998)
17. J. P. Colinge, X. Baie, V. Bayot, *IEEE Ele. Dev. Lett.*, **15**, 193-195 (1994)